



# Synthesis of $Y_3Al_5O_{12}:Eu^{3+}$ phosphor by sol-gel method and its luminescence behavior

Shen-Kang Ruan<sup>a</sup>, Jian-Guo Zhou<sup>a,b,\*</sup>, Ai-Min Zhong<sup>a</sup>, Jie-Fei Duan<sup>a</sup>, Xian-Bi Yang<sup>a</sup>, Mian-Zeng Su<sup>a</sup>

<sup>a</sup>Department of Chemistry, Peking University, Beijing, 100871, China

<sup>b</sup>Department of Chemistry, Henan Normal University, Xinxiang, 453002, China

## Abstract

The  $Eu^{3+}$ -doped  $Y_3Al_5O_{12}$  phosphor ultrafine powders were synthesized by the sol-gel method using metal alkoxide at the lower temperature of 1000°C. The formation process and structure of the phosphor powders were investigated by means of TG-DTA, XRD and SEM. It has been found that the phosphor powders were amorphous up to 700°C and changed into the single phase YAG at about 1000°C, that is, 600°C lower than that required for the constituent oxide mixtures. The resulting ultrafine, phase-pure, cubic yttrium aluminum garnet (YAG) phosphor powders were obtained. In the course of the phosphor transformation from non-crystalline state to crystalline state, both the emission intensity and the site symmetry of  $Eu^{3+}$  in the phosphors varied noticeably. The  $Eu^{3+}$  emission intensity of  ${}^5D_0 \rightarrow {}^7F_1$  and  ${}^5D_0 \rightarrow {}^7F_2$  versus  $Eu^{3+}$  concentration and sintering temperature was studied. © 1998 Elsevier Science S.A.

**Keywords:** Metal alkoxide; Sol-gel method; YAG-based phosphor; Luminescence behavior

## 1. Introduction

Yttrium aluminates are interesting compounds, in particular with regard to their optical properties. The phase equilibrium of the  $Y_2O_3$ - $Al_2O_3$  system has been studied extensively and the existence of three different kinds of crystal phases,  $Y_4Al_2O_9$  (YAM),  $YAlO_3$  (YAP) and  $Y_3Al_5O_{12}$  (YAG) has been reported in the literature [1]. YAG, the most important of these compositions, is well known as host material for a number of phosphor systems. Activation by  $Ce^{3+}$ , for example, gives a fast-response flying-spot scanner phosphor, and activation by  $Tb^{3+}$  gives a characteristic narrow-band phosphor suitable for contrast-enhanced display applications in high ambient illumination conditions [2]. The YAG lattice is resistant to degradation under the incident electron beam. Since high concentrations of certain trivalent rare earth (RE) ions can be substituted for  $Y^{3+}$  without concentration quenching [3], the phosphors are more linear.

The YAG-based materials are normally synthesized at a relatively high temperature (>1500°C) by a solid-state reaction between  $Al_2O_3$  and  $Y_2O_3$ . Such conditions normally lead to powders of relatively large and wider-varying grain sizes and varying impurity content. There are

often problems obtaining phase-pure material because of the intermediate formation of other phases, such as YAM and YAP, during the YAG synthesis [4]. A percentage of impurity unfavorably influences the optical properties based on YAG. The sol-gel method, because of its apparent advantages of fine homogeneity, high reactivity of starting materials and lower sintering temperature, is a new route to synthesizing fine powders. It has attracted more and more attention [5–8].

In this study, the  $Eu^{3+}$ -doped YAG phosphor precursors were synthesized by a sol-gel method using metal alkoxide. The high-purity, homogeneous, stoichiometric and ultrafine  $Eu^{3+}$ -doped  $Y_3Al_5O_{12}$  phosphor powders were obtained at a low temperature of 1000°C, which is 600°C lower than that required for the constituent oxide mixtures. The preparation of the gel precursors is described. The thermal decomposition, crystalline-phase compositions, particle size, morphologies and optical properties of the synthesized powders were evaluated.

## 2. Experimental details

### 2.1. Synthesis of the starting materials

Yttrium europium 2-methoxyethoxide was synthesized

\*Corresponding author.

as follows. Different amounts of  $Y_2O_3$  and  $Eu_2O_3$  (99.99% pure) were dissolved completely with concentrated HCl and evaporated to dryness in order to remove the surplus HCl. The obtained rare earth chlorides were dried by vacuum [9], then dissolved in an appropriate amount of dried  $CH_3OCH_2CH_2OH$ , to which was added sodium 2-methoxyethoxide under reflux. The process led to the formation of yttrium europium 2-methoxyethoxide and NaCl. The final compound could be separated by centrifugation.

## 2.2. Synthesis of the samples

The samples were synthesized by a sol-gel process using metal alkoxide. A 2.042 g amount of aluminum isopropoxide [10] was dissolved in 15.0 ml of dried isopropanol at 60°C, and 5–8 ml of ethanol was added to this solution while stirring. Then 13.1 ml of a 0.4583 mol  $dm^{-3}$  solution of yttrium europium 2-methoxyethoxide was added dropwise to the solution while stirring vigorously. An 0.8 ml volume of a 0.2 mol  $dm^{-3}$  solution of acetic acid ( $CH_3COOH$ ) and 1.0 ml of deionized water dissolved in ethanol was then added dropwise to the solution while stirring vigorously. The precursor solution was vigorously stirred at 80°C for an additional 4 h. The mole ratios of the metal alkoxide to solvent isopropanol, water and HAC were about 1:15~20:4~5:0.002. All of these operations were done in a dry  $N_2$  atmosphere. The precursors were left to gel at ~30°C, and the gels were put into a drying oven at ~80°C to form white gel powders. The dried gel powders were sintered in a loosely sealed quartz crucible in air. In order to analyze the intermediate products at various temperatures in the sintering process, the crucible was taken out of the furnace after a 3 h sintering and quenched immediately to room temperature. The quenching temperatures were at intervals of 50°C from 500°C to 1000°C.

## 2.3. Characterization of samples

### 2.3.1. The thermal analysis of precursor

The oven-dried precursor gel powders were investigated by thermogravimetric (TG) analysis and differential thermal analysis (DTA). Approximately 5.6 mg of the precursor gel powders were loaded into a standard platinum boat, which was heated from room temperature to 950°C at a constant heating rate of 10°C/min in a flowing air atmosphere.

### 2.3.2. Intermediate product analysis

The intermediate and final products formed in the sintering processes were analyzed by X-ray diffraction using  $Cu K\alpha$  radiation.

### 2.3.3. Phosphor morphology

The phosphor particle morphology was analyzed using scanning electron microscope (SEM) photographs.

### 2.3.4. Photoluminescence measurement

The excitation and emission spectra of samples were recorded using a Hitachi 850 spectrofluorometer. All of the measurements were carried out at room temperature.

## 3. Results and discussion

### 3.1. Formation of $YAG:Eu^{3+}$ in the sintering process

The TG and DTA curves of the thermal degradation of the oven-dried gel powders, which had a nominal composition of  $Eu_{0.12}Y_{2.88}Al_5O_{12}$  upon decomposition, are shown in Fig. 1. There are three stages of weight loss: (1) initial weight loss resulting from the evaporation of alcohol and desorption of the adsorbed moisture. The endothermic reactions and weight loss are observed up to 220°C; (2) decomposition of the organic compounds. The exothermic reactions and accompanied weight loss are observed at 220 to 400°C; (3) pyrolysis of the residual organics. The exothermic reactions and associated weight loss observed above 750°C result from the pyrolysis of the residual organics and crystallization of the gel, as indicated by the X-ray diffraction analysis results shown in Fig. 2. The total weight loss amounts to 44.87% for the dried-gel precursor. X-ray diffractograms for the decomposition products of the gel precursor for different sintering temperatures are shown in Fig. 2. The dried gel and powders obtained after heating to 700°C are X-ray amorphous. The YAM, as an intermediate product, appears first, as the sintering temperature is increased. Further heating leads to the formation of YAG at about 850°C, and then the intermediate products are changed into the single-phase crystallinity of cubic YAG ( $a=1.203$  nm) at about 1000°C, that is, about 600°C lower than required for the constituent oxide mixtures. Thus, the garnet phase formation was signifi-

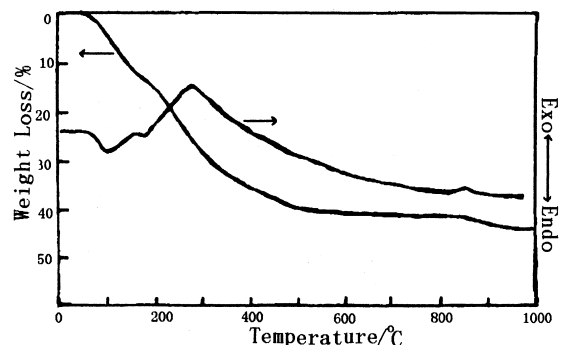


Fig. 1. DTA-TGA curves of  $Eu_{0.12}Y_{2.88}Al_5O_{12}$  gel precursor powder dried at 80°C.

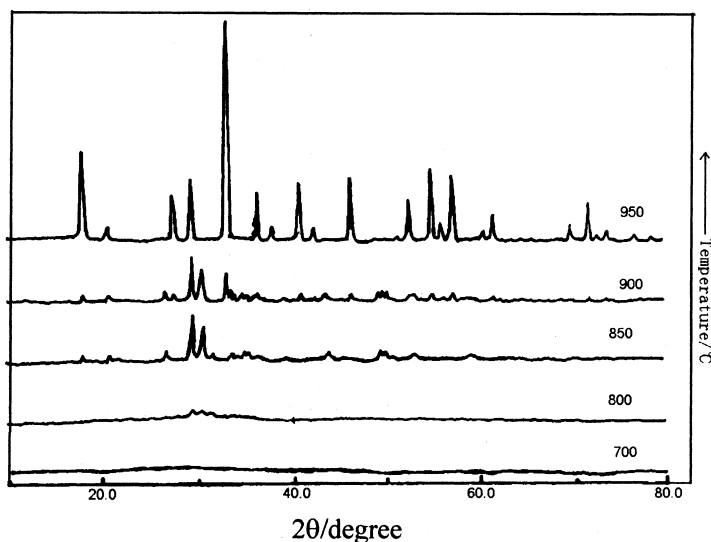


Fig. 2. XRD patterns of the  $\text{Eu}_{0.12}\text{Y}_{2.88}\text{Al}_5\text{O}_{12}$  dried gel precursor and its decomposition products.

cantly enhanced by the homogeneous mixing of the precursor powder in the gel sample.

### 3.2. Phosphor morphology

In Fig. 3 the SEM photographs of the quenched samples are shown. In the samples, at a sintering temperature of 500°C, the aggregates remained. Some of the aggregates had become single particles in the sample sintered at 700°C, and the monodispersed particles were obtained at 900°C. The particles are basically spherical in shape, the particle size is well distributed, and the radius is about 300 nm. These fine particles had grown as the sintering temperature increased.

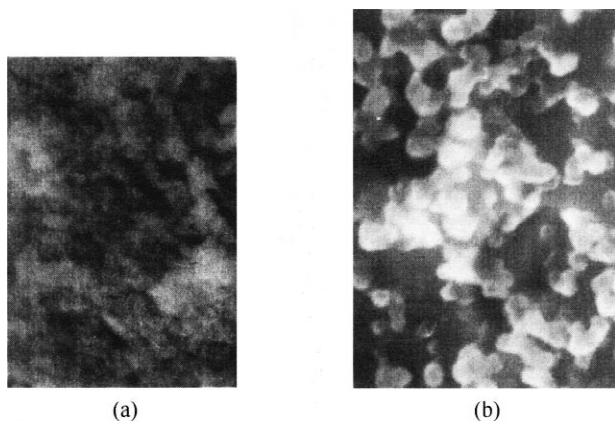


Fig. 3. SEM images of  $\text{Eu}_{0.12}\text{Y}_{2.88}\text{Al}_5\text{O}_{12}$  gel precursor sintered at (a) 500°C and (b) 900°C.

### 3.3. The influence of sintering temperature on luminescent properties of $\text{YAG}:\text{Eu}^{3+}$ phosphor

The  $\text{Eu}^{3+}$  emission intensity of the  ${}^5\text{D}_0 \rightarrow {}^7\text{F}_1$  and  ${}^5\text{D}_0 \rightarrow {}^7\text{F}_2$  transitions as a function of sintering temperature is shown in Fig. 4, for which the  $\text{Eu}^{3+}$  concentration was 0.6 mol %. From Fig. 4 it can be seen that the  ${}^5\text{D}_0 \rightarrow {}^7\text{F}_2$  emission is most intense up to 900°C, indicating a non-centrosymmetrical environment for the rare earth ions. The  ${}^5\text{D}_0 \rightarrow {}^7\text{F}_1$  emission intensity increases with increasing sintering temperature, it becomes the predominant as the sample was sintered at 1000°C, indicating that the  $\text{Eu}^{3+}$  ions lie in centrosymmetrical sites. The emission intensity ratios between the transition of  ${}^5\text{D}_0 \rightarrow {}^7\text{F}_1$  and  ${}^5\text{D}_0 \rightarrow {}^7\text{F}_2$

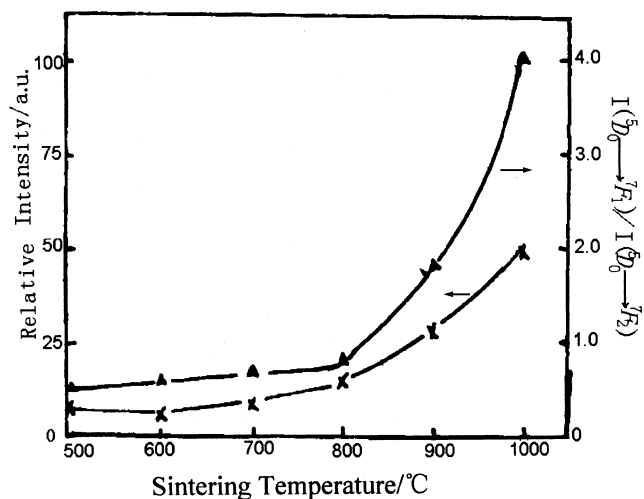


Fig. 4. Influence of sintering temperature on the emission intensity of  $\text{Eu}^{3+}$  in  $\text{Eu}_{0.12}\text{Y}_{2.88}\text{Al}_5\text{O}_{12}$ .

increase with increasing sintering temperature. They may be explained by the mixture ratio of YAM and YAG, and their crystallinity in the samples sintered at various temperatures. Furthermore,  $\text{Eu}^{3+}$  may be distributed differently in YAM. Thus, we may conclude that single-phase crystallinity of cubic  $\text{YAG}:\text{Eu}^{3+}$  is a key factor in luminescence efficiency.

### 3.4. Photoluminescence spectra

In Fig. 5 the emission of  $\text{Eu}^{3+}$  in  $\text{Y}_{2.88}\text{Eu}_{0.12}\text{Al}_5\text{O}_{12}$ , sintered both at 500°C and 1000°C under 395 nm excitation, is shown. The fluorescence of  $\text{Eu}^{3+}$  in  $\text{Y}_3\text{Al}_5\text{O}_{12}$  occurs mainly in the transitions of  ${}^5\text{D}_0 \rightarrow {}^7\text{F}_1$ . The spectra energy distributions of  $\text{Eu}^{3+}$  emission strongly depend on the  $\text{Eu}^{3+}$  concentration, as can be seen in Fig. 5. Variation of intensity emission of  ${}^5\text{D}_0 \rightarrow {}^7\text{F}_2$  transition versus concentration shows the absence of extinction, and the emission wavelength does not vary with the  $\text{Eu}^{3+}$  concentration. But the spectral shapes and emission intensity ratio between the transitions of  ${}^5\text{D}_0 \rightarrow {}^7\text{F}_1$  and  ${}^5\text{D}_0 \rightarrow {}^7\text{F}_2$  vary with the sintering temperature. The magnetic dipole transitions are predominant for the phosphor sintered at 1000°C, indicating the  $\text{Eu}^{3+}$  ions lie in centrosymmetrical sites. The absence of the  ${}^5\text{D}_0 \rightarrow {}^7\text{F}_0$  transition that occurs for a linear crystal field at the  $\text{Eu}^{3+}$  site, can also be noticed. Even in the dilute samples the emission from the  ${}^5\text{D}_1$  level is not observed, as expected from the high photon energies.

The excitation spectrum of the  $\text{Eu}^{3+} {}^5\text{D}_0 \rightarrow {}^7\text{F}_1$  emission for the composition  $\text{Y}_{2.88}\text{Eu}_{0.12}\text{Al}_5\text{O}_{12}$  sintered at 1000°C is given in Fig. 7. The  $\text{Eu}^{3+} 4f-4f$  transitions are very weak due to the fact that the electric dipole transitions are forbidden. The strongest sharp peak is at 395 nm which corresponds to  ${}^5\text{F}_0 \rightarrow {}^5\text{L}_6$  electronic transition of  $\text{Eu}^{3+}$  ion.

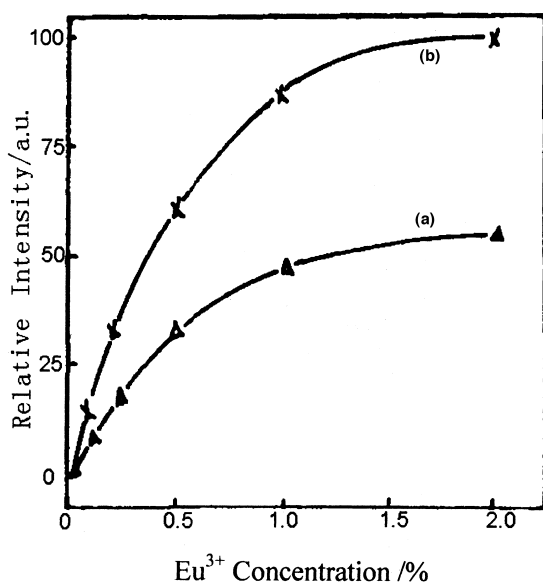


Fig. 5. The emission spectrum of the phase  $\text{Eu}_{0.12}\text{Y}_{2.88}\text{Al}_5\text{O}_{12}$  sintered at 500°C (a) and 1000°C (b).

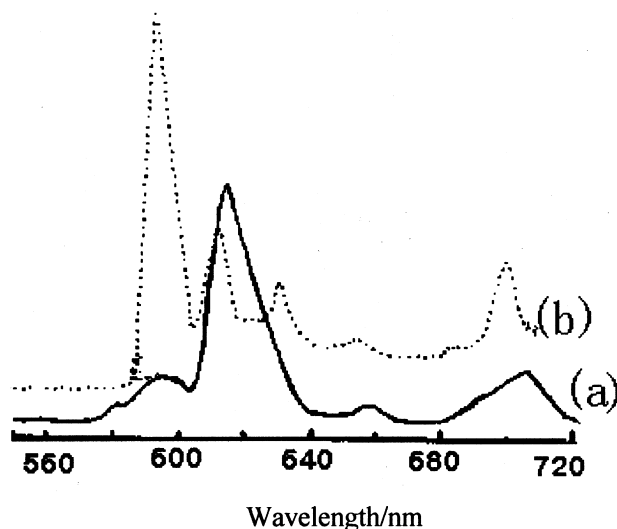


Fig. 6. Variation of the emission intensity of  $\text{Eu}^{3+}$  as a function of  $\text{Eu}^{3+}$  concentration.

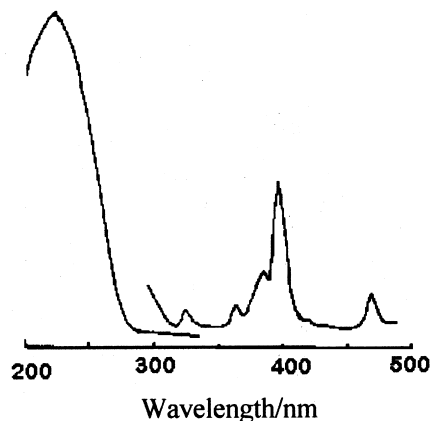


Fig. 7. The excitation spectrum of  $\text{Eu}^{3+}$  (0.6%) in YAG sintered at 1000°C.

The charge transfer (CT) band lies between 210 and 300 nm, to which the maximum is near 220 nm.

### References

- [1] J.S. Abell, I.R. Harris, B. Cockayne, et al., *J. Mater. Sci.* 9 (1974) 527.
- [2] G. Blasse, A. Bril, *Phys. Lett.* 11 (1967) 53.
- [3] D.J. Robbins, B. Cockayne, et al., *Phys. Rev.* 19 (1979) 1254.
- [4] K. Ohno, T. Abe, *J. Electrochem. Soc.* 133 (1986) 638.
- [5] S.J.L. Riberio, R.S. Hiratsuka, S.M.G. Massabni, et al., *J. Non-Cryst. Solids* 147–148 (1992) 162.
- [6] Sumiro Sakka, Toshinobu Yoko, *J. Non-Cryst. Solids* 147–148 (1992) 395.
- [7] Bulent E. Yoldas, *J. Non-Cryst. Solids* 147–148 (1992) 614.
- [8] H. Dislich, *J. Non-Cryst. Solids* 80 (1986) 115.
- [9] Su Mian-Zeng, Li Gen-Pei, *Huaxue Tongbao (Chemistry)* 4 (1979) 34.
- [10] E.L. Amma, *J. Inorg. Nucl. Chem.* 25(7) (1963) 779.